EBG-Based Self-Interference Cancellation to Enable mmWave Full-Duplex Wireless

Adewale K. Oladeinde, Ehsan Aryafar, and Branimir Pejcinovic
Portland State University, Portland, OR, USA

***Abstract*—Full-duplex (FD) wireless is a new technology that allows a wireless device to transmit and receive at the same time and on the same frequency. The key challenge to FD is self-interference (SI): a node's transmitting signal generates significant interference to its own receiver. Recent works have proposed several techniques to reduce SI and enable FD but they are primarily specific to sub-6 GHz frequency bands. In this paper, we focus on mmWave frequencies and propose to design the antennas in a way that they reduce SI. In particular, we design a novel electromagnetic band gap (EBG) architecture and integrate it with the antenna array to reduce SI. Extensive simulations show that the proposed design reduces SI by more than 60 dB over 100 MHz of isolation bandwidth at 28 GHz frequency. We also show that the design has minimal impact on the antenna array gain, maintains the gain over large bandwidth, and has a return loss similar to a design with no EBG.**

***Index Terms*—Full-duplex wireless, MmWave communication, Self-interference, Electromagnetic band gap**

I. Introduction

Millimeter-Wave communication is a promising technology for future broadband wireless networks. While originally designed for semi-stationary applications such as wireless docking and cellular backhaul [1], mmWave communication is nowadays a key component of 5G and can provide high capacity mobile data rates [2].

mmWave systems are typically associated with large bandwidthds, e.g., a typical 802.11 ad[1] device routinely uses 2 GHz of bandwidth in the 60 GHz band for communication. However, the amount of mmWave spectrum available to cellular operators depends on the locality and could be far less. For example, even after the recent FCC 5G spectrum auctions [4], AT&T (the second largest mmWave spectrum holder in the US) holds only an average of 630 MHz of mmWave bandwidth [5] in the top 100 PEAs [2]. In addition, AT&T's initial mmWave deployments use only 100 MHz of bandwidth [7]. With mobile data traffic expected to double each year [8], it is therefore imperative to seek solutions that increase the spectral efficiency of mmWave systems.

Full-duplex (FD) wireless is an emerging solution in this direction, which can double the physical layer spectral efficiency by eliminating self-interference (SI). With FD, transmission and reception happen on the same time-frequency resource block unlike existing FDD/TDD wireless systems.

FD wireless has been extensively studied over the past decade but majority of the research is dedicated to sub-6 GHz frequency bands [9], [10]. To enable FD, a large amount of SI need to be cancelled. For example, to build a FD WiFi radio with 20 dBm transmission power and -90 dBm noise floor, 110 dB of SI needs to be cancelled. Existing techniques remove the SI at multiple stages, e.g., SI can be initially removed through passive cancellation (e.g., specific antenna design), then possibly with active RF/analog cancellation, and finally through digital cancellation, which removes the remaining SI that cannot be cancelled through passive and active RF cancellation in the digital baseband.

More recently, the community has started to tackle the problem of mmWave FD radio design. CMOS RF cancellation techniques have been proposed in [11], [12], however, these designs are all limited to a small number of antennas (e.g., 1 transmit and 1 receive antenna). Real-world mmWave radios, on the other hand, use an array of antennas to increase the beamforming gain and compensate for the high path loss associated with mmWave frequencies. Our goal in this paper is to study whether SI can be reduced as part of the mmWave antenna design. In particular, we design a novel electromagnetic band gap (EBG) structure coined "VicCross", which is integrated in the antenna substrate, and evaluate its performance in terms of SI reduction, antenna gain, and bandwidth of operation. Our key contributions are as follows:

- **Design:** The key idea behind our design is to separate the Tx and Rx antenna arrays and integrate the substrate between them with VicCross EBG with bow-tie slots to reduce the SI power. We show that the design effectively reduces the surface wave electric field power between the Tx and Rx arrays. We also derive a circuit model that shows the VicCross EBG with bow-tie slot on the ground plane creates a high impedance path between the Tx and Rx arrays.
- **Evaluation:** We conducted extensive simulations using High Frequency Structure Simulator (HFSS [13]) to evaluate VicCross EBG. We show that with a combination of bow-tie slot on the ground plane and VicCross EBG between the Tx and Rx antenna arrays, we can achieve up to -70 dB of Tx-Rx isolation at 28 GHz with more than 100 MHz of isolation bandwidth at -60 dB. We also show that VicCross EBG provides up to 20 dB more isolation compared to a conventional mushroom EBG optimized for operation in the 28 GHz band. Finally, we show that VicCross EBG has negligible impact on other antenna performance metrics such as antenna gain, frequency bandwidth, and return loss.

[1]WiFi mmWave standard [3].

[2]PEA: Partially Economic Area, which is a unit of area used by FCC in assigning radio licenses [6].

978-0-7381-1299-2/21/$31.00 ©2021 IEEE

The rest of this paper is organized as follows. We describe the antenna considered in this paper in Section II. Antenna array configuration and EBG integration is discussed in Section III. We present the results of our extensive simulations in Section IV. Finally, we conclude the paper in Section V.

II. Antenna Design Configuration

We consider a wireless device with separate transmit (Tx) and receive (Rx) antenna arrays for the following reasons: (i) antenna separation reduces SI by up to 40 dB as we show through simulations in Section IV; (ii) circulator based systems are ill-suited at mmWave frequencies due to larger size and inability to scale to multi-antenna systems, and (iii) smaller antenna sizes at mmWave bands allow us to pack more arrays in the same wireless device.

Each Tx/Rx antenna array studied in this paper is composed of four 1x4 series fed patch antennas spaced at 0.5λ (where λ denotes the wavelength) as shown in Fig. 1. The Tx and Rx antenna arrays are designed and optimized on the same substrate system with 1.6λ edge-to-edge distance. The 1.6λ distance is chosen as a compromise between array port to port coupling and size of the system we considered for this application[3]. Each antenna array is optimized for maximum array gain using HFSS full-wave electromagnetic simulation tool. Rogers RO3035 substrate material with thickness of 50 μm along with permittivity and loss tangent values of 3.6 and 0.0015 was employed [14]. Two adjacent patch elements in a 1x4 series fed array are connected using 0.1λ electrical length of transmission line. The first three patch were designed using edge feed while the top patch is designed using inset feed. The first two lower patches have the same width of 0.36λ along with lengths of 0.36λ and 0.45λ, respectively. The two top patches are square shaped with width and length of 0.4λ. The length and width of each patch were determined using Eqs. (1)-(3) [15]:

$$W = \frac{v_0}{2f_r}\sqrt{\frac{2}{\varepsilon_r}} \tag{1}$$

$$L = \frac{1}{2f_r\sqrt{\varepsilon_{reff}}\sqrt{\mu_0\varepsilon_0}} - 2\Delta L \tag{2}$$

$$\Delta L = 0.412 \times \frac{(\varepsilon_{reff}+0.3)(\frac{W}{h}+0.264)}{(\varepsilon_{reff}-0.258)(\frac{W}{h}+0.8)} \tag{3}$$

here, w, L, and ΔL denote the patch width, patch length, and patch length extension, v_0 is the speed of light in free space, ε_r, ε_0, ε_{reff}, μ_0, and h are relative permittivity, permittivity of free space, effective permittivity, permeability, and thickness of the substrate material, and f_r denotes the resonant (desired) frequency. In this paper, we set f_r to 28 GHz[4].

[3]We considered a portable wireless device application such as a smartphone.

[4]We have recently acquired a 5G software-defined radio, which operates in the 28 GHz band and allows us to experiment with different antenna designs. As part of our future work, we plan to compare the results of the simulations presented in this paper with experiments conducted on our 5G hardware.

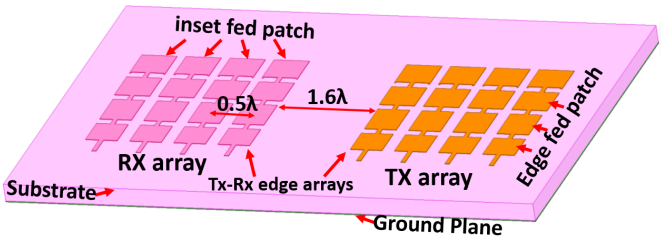

Fig. 1. 4x4 Tx and Rx antenna arrays on the same substrate material separated by 1.6λ. The location of edge 1x4 Tx-Rx arrays are also specified. The impact of SI is most sever between the two edge arrays due to their proximity.

The input ports to the 4x4 array for both the transmitter and receiver antenna array are all excited to transmit and receive signals at same time to mimic FD communication. Further, each individual port is designed to be fed with an independent phase shifter to mimic a phased array system. The results of array coupling analysis (simulation) or transmit and receive signal interference isolation investigated in this paper (Section IV) uses the closest two 1x4 arrays, one from the transmitter and one from the receiver antenna array. These edge arrays have the worst case coupling characteristics (i.e., have the highest SI). The total coupling coefficient seen by an edge 1x4 array for the transmitter (receiver) array is a summation of the mutual and self coupling coefficients of the 4x4 transmitter (receiver) array.

III. EBG Integration in Antenna Array

Electromagnetic band-gap (EBG) structure is a structure that creates a stopband to block electromagnetic waves of certain frequency bands by forming a fine, periodic pattern of small metal patches on dielectric substrates. EBG refers to such a stopband as well as to substances (medium to transmit electromagnetic waves) that have such a structure. Applications of the EBG structure include components of electronic devices to suppress electromagnetic noise as well as design of antenna and other microwave circuits [16]. More recently, a conventional mushroom EBG has been used to reduce SI and enable FD at 3.2 GHz frequency band [17]. In this paper, we develop a new EBG design targeted for mmWave frequencies (28 GHz) and extensively evaluate its performance through simulations.

A. Mushroom EBG Design and Its Integration with the Tx and Rx Antenna Arrays

We start by designing a mushroom EBG composed of metallic square patches with unit element width and air-gap size of 4 mm and 3.4 mm, respectively. The EBG is designed for a stop band at 28 GHz as shown in Fig. 2. Here, the blue line shows the transmission loss (S_{12}) of a transmission line using a solid ground plane as its return path. The red curve shows the transmission loss when EBG is employed.

Eqs. (4)-(6) [15] guided our design of the mushroom EBG:

$$C = \frac{W\varepsilon_0(1+\varepsilon_{reff})}{\pi}\cosh^{-1}(\frac{W+g}{g}) \tag{4}$$

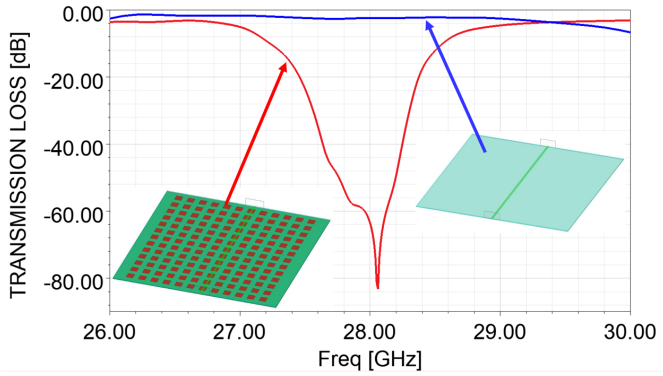

Fig. 2. Blue curve with close to zero loss shows the transmission loss (S_{12}) of a transmission line using a ground plane as its return path. The red curve shows the transmission loss when mushroom EBG is employed.

$$L = 2 \times 10^{-7} \times h \times [\ln(\frac{2h}{r}) + 0.5(\frac{2r}{h}) - 0.75] \quad (5)$$

$$f = \frac{1}{2\pi\sqrt{LC}} \quad (6)$$

here W is the unit element width, g is the gap between two EBG unit elements, ϵ_0 and ϵ_{reff} are free space and relative permittivity of substrate material, h is the substrate material thickness, r is the radius of EBG shorting via, L, C and f are the inductance, capacitance, and resonant frequency of the EBG design.

The initial mushroom design derived from the above theoretical formulas was further optimized in HFSS to provide maximum isolation of up to -80dB at 28GHz frequency.

Fig. 3 shows the integrated mushroom EBG with the 4x4 Tx and Rx antenna arrays. The mushroom EBG patch was further optimized to obtain Tx-Rx isolation (SI reduction) of up to -48dB at 28GHz as we will show later through simulations in section VI.

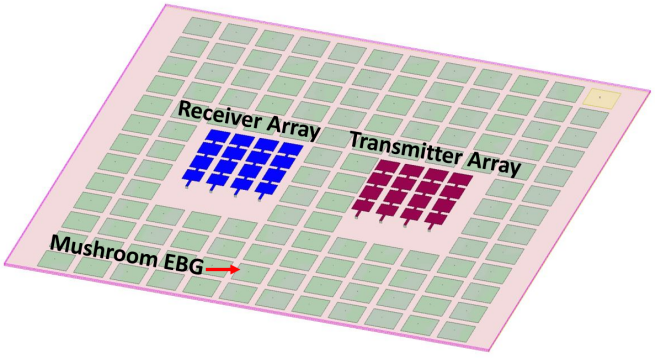

Fig. 3. Mushroom EBG integrated with 4x4 Tx and Rx antenna arrays.

B. VicCross EBG and Ground slot, and Their Integration with the Tx and Rx Antenna Arrays

The mushroom EBG metallic patch was further optimized and modified by cutting slots on the patch to increase inductance and reduce capacitance to form a new EBG design coined "VicCross EBG". We chose the name VicCross due to its shape's similarity to a Victorian Cross as shown in Fig. 4.

The VicCross geometry (Fig. 4, top right hand side) consists of a metal sheet with a two-dimensional lattice of resonant elements, acting as a two dimensional filter to prevent the propagation of electric current.

VicCross EBGs with bow-tie cross slot on the ground plane (Fig. 4, top left hand side) were used between transmit and receiver antenna arrays, while VicCross with shorting via to ground plane were used to surround the antenna arrays (Fig. 4, buttom). We will later show in Section IV that the proposed EBG provides up to 20 dB of additional isolation (SI reduction) compared to the mushroom EBG.

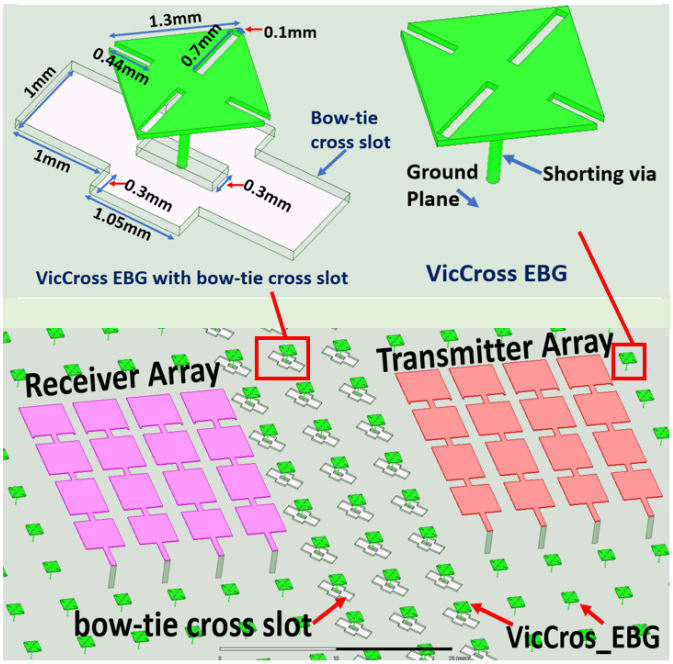

Fig. 4. 4x4 TX-RX antenna arrays integrated with VicCross EBG. VicCross EBG with bow-tie cross slots are integrated between the Tx and Rx antenna arrays. VicCross EBG also surrounds the two arrays in a periodic manner.

The electromagnetic wave from Tx to Rx antenna array propagates through two paths: the ground plane and the substrate. Our design reduces the coupling in both paths.

The bow-tie cross slot on the ground plane was designed as a defective ground structure between the transmit and receive array elements in order to increase the inductive path of the electromagnetic wave coupling on the ground plane. Further, VicCross EBG between Tx and Rx array element is designed to have series capacitance to the ground loop inductance in order to further reduce the capacitance of VicCross EBG patch to the ground plane. A circuit model shown in Fig. 5 can be used to describe the lumped element behaviour.

From the equivalent circuit model in Fig. 5, at frequencies below the design frequency, the circuit model becomes inductive and supports TM surface waves, whereas at frequencies above the design frequency, the circuit model becomes capaci-

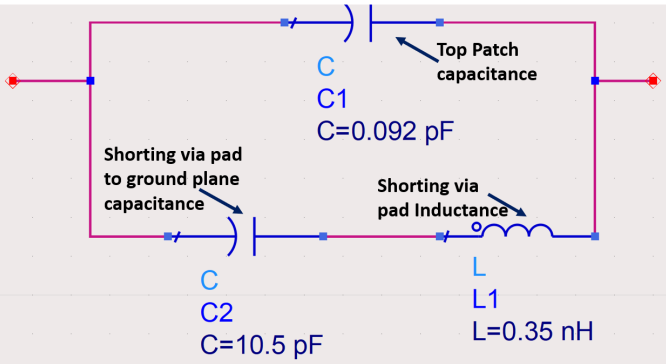

Fig. 5. VicCross EBG surface impedance circuit model. The component values are reported by the ADS (Advanced Design Suite) software (developed by Keysight), which approximate the VicCross EBG model.

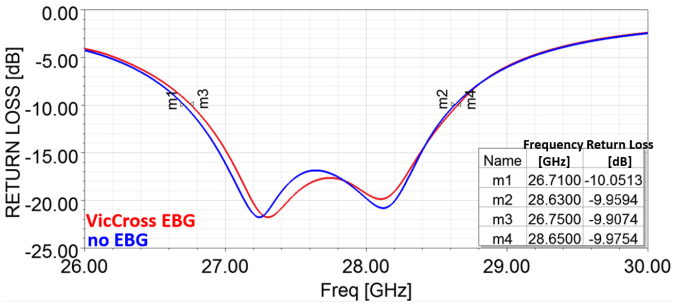

Fig. 6. Active s-parameter plot showing VicCross EBG and noEBG frequency bandwidth at -10dB return loss.

tive and thereby supports TE surface waves. At a narrow band around the LC resonance point (frequency), the impedance between the Tx and Rx antenna arrays becomes very high.

The VicCross EBG is designed so that its surface wave band gap covers our desired antenna resonant frequency bandwidth.

Note that, as shown in Fig. 4, there is no EBG structure under the antenna arrays. Further, the thickness of the substrate under the antenna arrays is the same as when EBG is not used. This is to keep the antenna frequency bandwidth of our design similar to the design with no EBG. The edge gap between the antenna array and surrounding VicCross EBGs is carefully chosen in order not to affect the frequency bandwidth of the antenna and to also effectively reduce the surface wave.

IV. Performance Evaluation

We characterize the performance of the VicCross EBG through extensive simulations using HFSS. As a baseline for comparison, we consider the antenna design with separate Tx and Rx antenna arrays but with no EBG (i.e., Fig. 1). We show that the VicCross EBG has only a minor impact on the antenna performance metrics (frequency bandwidth, gain) but substantially increases the Tx-Rx isolation (i.e., substantially reduces the SI power). We end our performance evaluation by demonstrating the electric field coupling between the Tx and Rx arrays.

Antenna Frequency Bandwidth. Fig. 6 shows the active S-parameter plot of 4x4 array ports. Active S-parameters [18] represent the reflection coefficients for the various 1x4 array excitations and is an important performance metric for active phased array antennas. Active S-parameter of transmitter and receiver edge ports (i.e., the two closest Tx and Rx 1x4 arrays) were plotted in Fig. 6 for both when EBG is not employed (blue curve) and when VicCross EBG with bow-tie ground slot is used (red curve). In each design, the Tx and Rx edge ports have a similar performance. As a result, each curve in Fig. 6 corresponds to either Tx or Rx edge ports. In antenna design, a return loss of -10 dB or lower is typically desirable. From Fig. 6, we observe that VicCross EBG has a 1.9 GHz impedance bandwith, which is only 20 MHz less than the impedance bandwidth when EBG is not employed.

Antenna Gain. Fig. 7 demonstrates the Tx (Rx) 4x4 antenna gain in both E and H planes. We observe that the VicCross EBG slightly increases the gain but narrows the beamwidth. We also observe up to 5 dB increase in side lobe level (SLL) and back side lobe which are due to the interaction of the reflected surface waves caused by the VicCross EBG, changes in electrical characteristics of the ground plane shape, and the antenna radiation characteristics. We hypothesize that a further optimization of the EBG placement near the antenna array could improve the SLL and back lobe performance. On the other hand, H-plane performance of the VicCross EBG and no EBG are quite similar.

We next plot the bore-sight gain variation across the frequency bandwidth in Fig. 8. We observe that VicCross EBG and no EBG exhibit a similar gain vs frequency performance. In both designs, a maximum gain of 18.5 dB is reached at 28 GHz, which remains the same as the frequency increases.

Tx-Rx Isolation (SI reduction). We next characterize the reduction in SI power for three scenarios: (i) no EBG, (ii) conventional mushroom EBG (discussed in Section II), and (iii) VicCross EBG with bow-tie slot. Fig. 9 shows the Tx-Rx isolation across the three schemes. We observe that even without EBG there is between -35 and -40 dB of Tx-Rx isolation, which is due to Tx-Rx antenna separation. The Mushroom EBG provides up to -48 dB of isolation at 28GHz as shown in the same figure, which is 13dB more isolation with antenna array with no EBG. We also observe that the mushroom EBG has a consistent performance as a function of frequency. Our proposed VicCross EBG with bow-tie cross slot provides up to -70 dB of isolation at the 28 GHz frequency with more than 100 MHz of isolation bandwidth at -60 dB [5]. At its maximum isolation point, this is 32 dB more isolation when compared to the no EBG antenna array and 20dB more isolation when compared to the antenna array with conventional mushroom EBG. Its important to note that the port to port isolation plots in Fig. 9 correspond to active s-parameter plots of the edge 1x4 Tx and Rx arrays, where the SI power is highest .

Tx-Rx Electric Field Coupling. We next investigate the

[5]Wireless applications that use this bandwidth will have Tx and Rx isolation of more than 60 dB. For example, AT&T's initial mmWave deployments use only 100 MHz of bandwidth [7]. Therefore, lower isolation at adjacent frequencies will not impact the performance of the FD communication link.

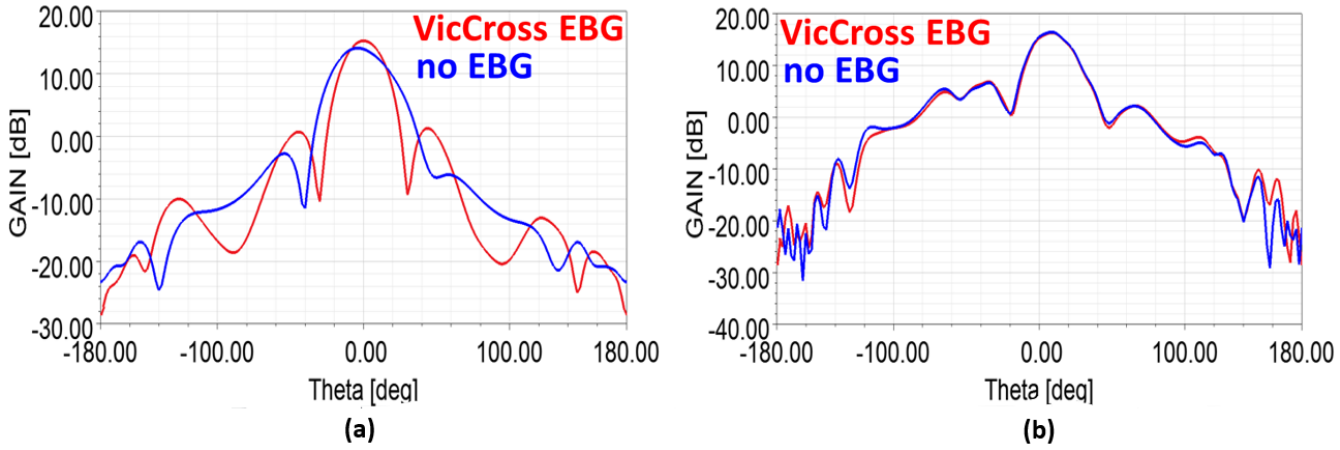

Fig. 7. (a): E-plane gain. VicCross EBG slightly increases the gain but narrows the beamwidth. We also observe up to 5 dB increase in side lobe level; (b) H-plane performance of the VicCross EBG and no EBG are quite similar.

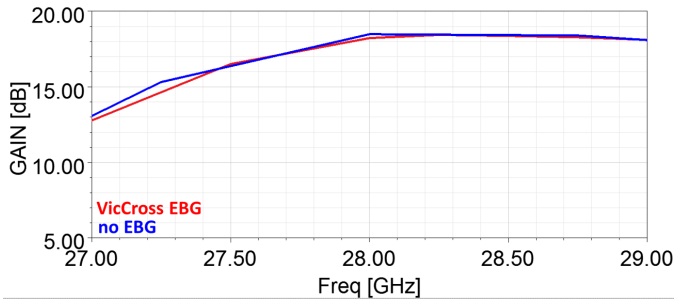

Fig. 8. Tx/Rx antenna array gain as a function of frequency. VicCross EBG has negligible impact on the antenna gain.

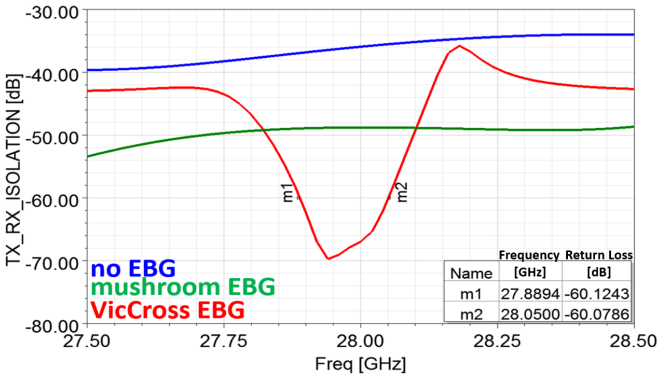

Fig. 9. Transmitter-Receiver isolation with no EBG (blue), with mushroom EBG (green) and VicCross EBG (red). VicCross EBG with bow-tie cross slot provides up to -70 dB of isolation at 28 GHz frequency with more than 100 MHz of isolation at -60 dB.

electric field coupling between the Tx and Rx antenna arrays resulting from the surface wave radiation through the substrate for both with and without EBG and plot them in Fig. 10. Our simulation in Fig. 10(a) shows a higher coupling of more than 57 dB(V/m) with no EBG, while Fig. 10(b) shows reduction in coupling down to 46 dB(V/m) between the VicCross EBG and the antenna array. The VicCross EBG interaction with the substrate material properties resulted in a high impedance path for the surface wave electric field to propagate from the Tx to Rx array.

V. Conclusion

We studied the problem of self-interference reduction to enable mmWave full-duplex wireless. Our key idea was to separate the Tx and Rx antenna arrays and integrate the substrate between them with VicCross EBG with bow-tie slots to reduce the SI power. We conducted extensive simulation using HFSS and showed that the design can achieve up to -70 dB of Tx-Rx isolation at 28 GHz with more than 100 MHz of isolation of bandwidth at -60 dB. We showed that VicCross EBG provides up to 20 dB more isolation compared to a conventional mushroom EBG optimized for operation in the 28 GHz band. We also showed that the design has negligible impact on other antenna performance metrics such as antenna gain and frequency bandwidth.

Acknowledgements

This research was supported in part by an NSF award (CNS-1942305).

References

[1] IEEE 802.11 Standard, "IEEE 802.11ad, amendment 3: Enhancements for very high throughput in the 60 GHz band," 2012.

[2] 5G PPP, "The 5G infrastructure public private partnership," in *https://5g-ppp.eu/*.

[3] T. Nitsche, C. Cordeiro, A. B. Flores, E. W. Knightly, E. Perahia, and J. C. Widmer, "IEEE 802.11ad: directional 60 GHz communication for multi-gigabit-per-second WiFi," in *IEEE Communications Magazine*, 2014.

[4] "5G Millimeter Wave Auction Winners: AT&T, T-Mobile, Verizon, Windstream, Starry, and Others," https://www.telecompetitor.com/5g-millimeter-wave-auction-winners-att-t-mobile-verizon-windstream-starry-and-others/.

[5] "AT&T Enhances Spectrum Position Following FCC Auction 102," https://about.att.com/story/2019/att_enhances_spectrum_position.html.

[6] "FCC list of Partial Economic Areas (PEAs)," https://www.fcc.gov/oet/maps/areas.

[7] "An evaluation of AT&T millimeter wave markets," https://www.allnetinsights.com/blogs/news/at-t-millimeter-wave-markets.

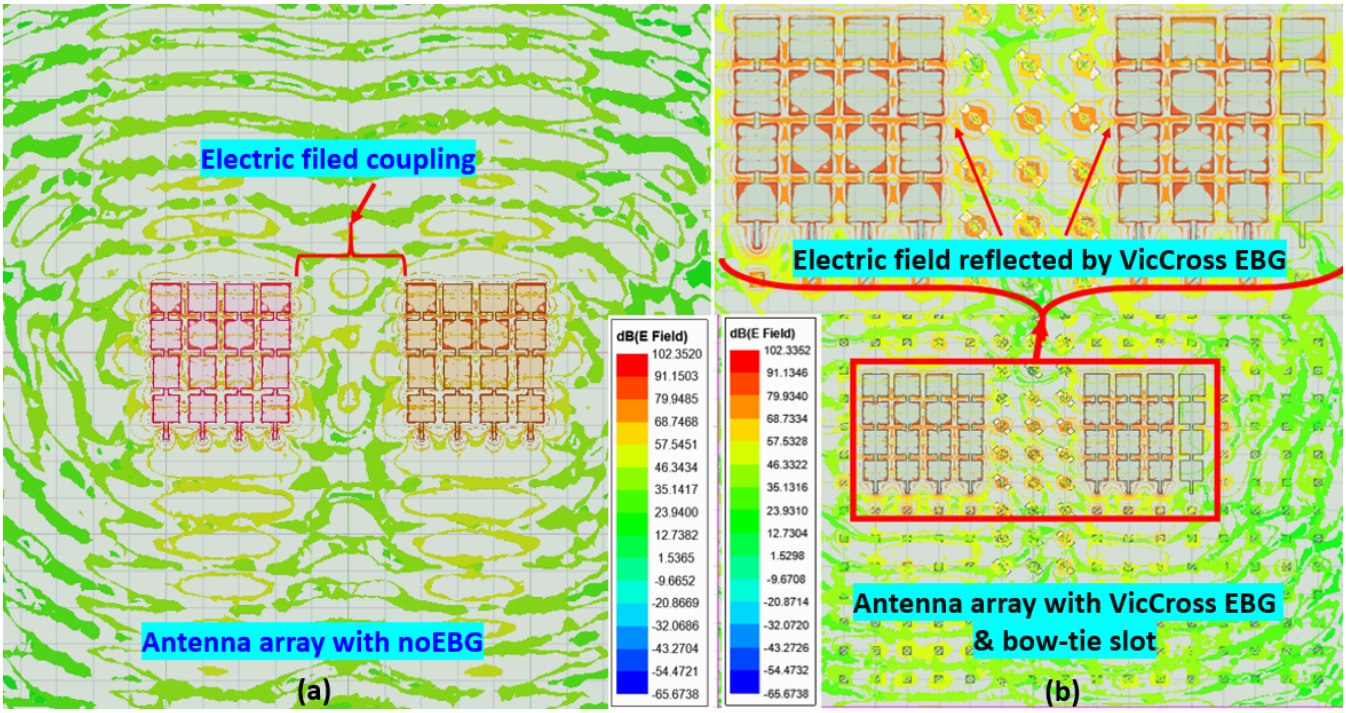

Fig. 10. (a): noEBG substrate Electromagnetic field propagation; (b) VicCross EBG substrate Electromagnetic field propagation. VicCross EBG reduces the coupling of up to 46 dB (V/m) between the EBG and antenna array.

[8] "Ericsson mobility report: on the pulse of yje networked society," https://www.gsma.com/latinamerica/ericsson-mobility-report-networked-society/.

[9] A. Sabharwal, P. Schniter, D. Guo, D. W. Bliss, S. Rangarajan, and R. Wichman, "In-band full-duplex wireless: challenges and opportunities," in *IEEE Journal on Selected Areas in Communications*, 2014.

[10] E. Aryafar and A. Keshavarz-Haddad, "PAFD: phased array full-duplex," in *Proceedings of IEEE INFOCOM*, 2018.

[11] N. Reiskarimian, M. B. Dastjerdi, J. Zhou, and H. Krishnaswamy, "Analysis and design of commutation-based circulator-receivers for integrated full-duplex wireless," in *IEEE Journal of Solid State Circuits*, 2018.

[12] J. Zhou, N. Reiskarimian, J. Diakonikolas, T. Dinc, T. Chen, G. Zussman, and H. Krishnaswamy, "Integrated full duplex radios," in *IEEE Communications Magazine*, 2017.

[13] "3D electromagnetic field simulator for RF and wireless design," https://www.ansys.com/products/electronics/ansys-hfss.

[14] "Ro3000 series circuit material: Ro3003, ro3006, ro3010 and ro3035 high frequency laminate," Available at: https://www.rogerscorp.com.

[15] F. Yang and Y. Rahmat-Samii, *Electromagnetic band gap structures in antenna engineering*, Cambridge University Press, New York, NY, USA, 2008.

[16] N. Kushwaha and R. Kumar, "Study of different shape electromagnetic band gap (ebg) structures for single and dual band application," in *Journal of Microwave, Optoelectronics and Electromagnetic Applications*, 2014.

[17] D. Mirshekar-Syahkal P.Deo and G. Zheng, "EBG Enhanced Broadband Dual Antenna Configuration for Passive Self-Interference Suppression in Full-Duplex Communications," in *Proceedings of the 48th European Microwave Conference*, 2018.

[18] "Active-s parameter measurement and plot in hfss," Available at: http://www.ece.uprm.edu/ rafaelr/inel6068/HFSS/hfss_onlinehelp.pdf.